Wall++: Room-Scale Interactive and Context-Aware Sensing

Yang Zhang[1,2] Chouchang (Jack) Yang[1] Scott E. Hudson[1,2] Chris Harrison[1,2] Alanson Sample[1]

[1] Disney Research Pittsburgh
4720 Forbes Ave, Suite 110, Pittsburgh, PA 15213
{jack.yang, alanson.sample}@disneyresearch.com

[2] Carnegie Mellon University
5000 Forbes Avenue, Pittsburgh, PA 15213
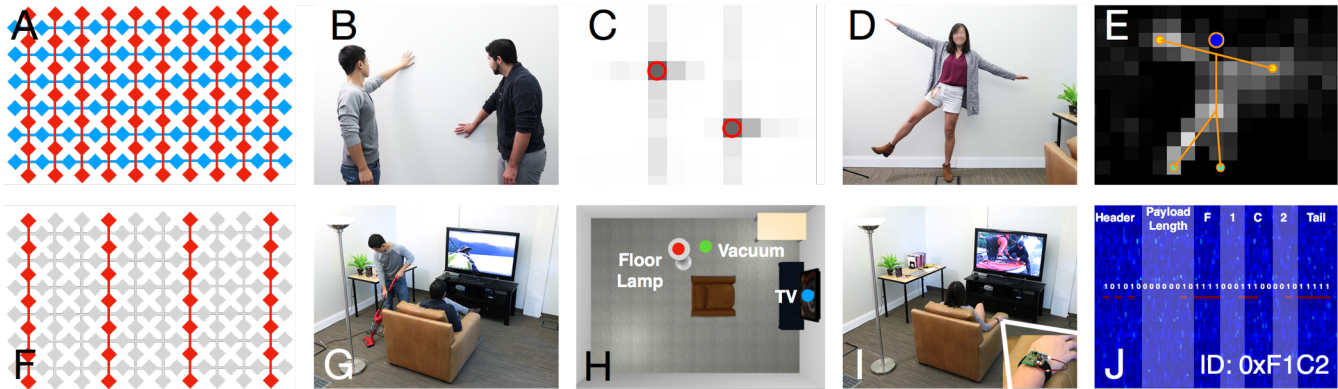{yang.zhang, scott.hudson, chris.harrison}@cs.cmu.edu

Figure 1. Wall++ in active mutual capacitive sensing mode (A) enables touch tracking (B,C) and pose estimation (D,E). Wall++ in passive airborne electromagnetic sensing mode (F) enables appliance detection and tracking (G,H), as well as user ID (I,J).

ABSTRACT

Human environments are typified by walls – homes, offices, schools, museums, hospitals and pretty much every indoor context one can imagine has walls. In many cases, they make up a majority of readily accessible indoor surface area, and yet they are static – their primary function is to be a wall, separating spaces and hiding infrastructure. We present Wall++, a low-cost sensing approach that allows walls to become a smart infrastructure. Instead of merely separating spaces, walls can now enhance rooms with sensing and interactivity. Our wall treatment and sensing hardware can track users' touch and gestures, as well as estimate body pose if they are close. By capturing airborne electromagnetic noise, we can also detect what appliances are active and where they are located. Through a series of evaluations, we demonstrate Wall++ can enable robust room-scale interactive and context-aware applications.

Author Keywords

Touch Sensing; Gestures; Pose Estimation; Indoor Localization; User Identification; Internet of Things; EM Sensing, Context Aware; Smart Environments.

ACM Classification Keywords

H.5.2. [User interfaces] – Input devices and strategies.

INTRODUCTION

Walls are everywhere, often making up more than half of indoor surface area, especially in residential and office buildings. In addition to delimiting spaces, both for functional and social purposes, they also hide infrastructure, such as wiring and HVAC. However, they are generally inactive structural elements, offering no inherent interactive or computational abilities (other than at small attached silos, e.g., thermostats and light switches), and thus present a tempting opportunity for augmentation, especially considering their ubiquity.

In this work, we set out to identify methods that could recast walls as smart infrastructure, able to sense interactions and activities happening in a room. In addition to supporting these broad application domains, we also added process constrains. In particular, we sought a technical approach that was *versatile* and *easy to apply*, requiring *no special tools* (e.g., CNC machines) or *skills* (e.g., carpentry, electrical engineering). We also required our approach to be *low-cost*, so as to be economically feasible at room scale (even a small room, e.g., 2×2.5×2.5 m, has more than 20 m^2 of walls). Finally, we wanted our sensing approach to be *minimally obtrusive*, and ideally invisible.

We quickly identified paint as a particularly attractive approach. Walls are already painted, and the average homeowner has the requisite skills to paint a wall. While there are special tools for applying paint (e.g., brushes, rollers, painter's tape), these are all commodity supplies and readily available at home improvement stores. As we will discuss in greater depth later, we can apply a standard latex topcoat, which allows our technique to be wall-scale, and yet hidden in plain sight. Our ultimately selected method costs ~$20

per m^2 in materials at retail prices. These properties satisfied all our process criteria.

To enable user and environmental sensing, we drew upon two large bodies of work in the literature. First, we selected mutual capacitive sensing [8,20,59,65] for close-range interactions. Owing to its widespread use in smartphones and tablets, mutual capacitive sensing is well understood and robust, allowing us to readily adapt it to wall-scale applications. Second, we extended work in airborne electromagnetic (EM) sensing [52,62,78,79]. This required us to develop an electrode pattern that supports both of these sensing modalities (Figure 1, A & F). For *user sensing*, we investigated touch interaction (Figure 1, B & C), pose estimation (D & E), user identification and tracking (I & J). For *environment sensing*, we focused on context awareness though appliance recognition and localization (G & H).

Collectively, we call our process, materials, patterns, sensor hardware and processing pipeline, Wall++. As we detail in the following pages, optimizing for ease-of-application and reliability, as well as sensing range and resolution, required iterative experimentation, physical prototyping, simulation modeling and user studies. We believe our resulting system demonstrates new and interesting HCI capabilities and presents a viable path towards smarter indoor environments.

RELATED WORK
Our work intersects with three key literatures. First, we discuss prior work that enables room-scale touch tracking. We then review room-scale approaches for tracking user location and pose. We conclude with systems able to detect and track objects. In particular, we focus primarily on systems that are deployed in the environment, as opposed to those that are carried (e.g., smartphones, wearables).

Room-Scale Touch
Most previous systems have achieved wall-scale touch sensing through optical approaches. For example, LaserWall [53] used a scanned laser rangefinder operating parallel to a wall's surface to detect hand touches. Infrared emitter-detector arrays have also been used to create large interactive surfaces [44]. Most popular are camera-based approaches, including invisible light [60], depth [7,30,74, 75,76], and even thermal imaging [37].

People have also explored acoustic touch sensing approaches, for example, by attaching microphones to the corners of a desired interactive surface and using time difference of arrival methods [29,54]. It is also possible to use an array of centrally located acoustic sensors for estimating the location of tap events [77]. Researchers have also forgone absolute spatial tracking, and instead built interactions around gesture vocabularies [27].

More relevant to Wall++ are systems that use capacitive sensing. Early work by Smith et al. [65] demonstrated a capacitive sensing wall able to detect user gestures such as swipes, though users had to stand on an active transmitter electrode. Living Wall [41] offered discrete touch patches

as part of an art installation. Electrick [81] used electrical field tomography for coarse touch tracking, including a demo on a 4×8' sheet of drywall. To enable fine-grained finger interactions on furniture, researchers have used dense, self-capacitive electrode matrices [10,51].

Most related to our work is SmartSkin [59], which demonstrated a table-sized (80×90 cm) mutual capacitive matrix for touch sensing. We move beyond this seminal work with novel hardware and tracking algorithms, as well as a deeper exploration of electrode/antenna fabrication, especially as it relates to walls. We also uniquely consider interaction modalities at room scale.

User Tracking and Pose Estimation
There is an extensive literature on indoor user localization (see [14,42] for an extended review). Technical approaches that instrument the environment include computer vision [63,68], floor pressure sensing [53], floor and/or furniture capacitive sensing [2,22,45,69], and RF sensing [73,80]. Conversely, users can be instrumented with tags, such as RFID [40,46] and Bluetooth beacons [26,32].

There has also been substantial work on human pose estimation. Most common is to use cameras looking out onto an environment [11]. Alternatively, cameras have been installed below the floor, as seen in GravitySpace [9] and MultiToe [5] which used a room-sized FTIR floor to track users and infer posture. Beyond cameras, RF-based approaches are also popular, including Doppler radar [57], RFID tracking [72] and co-opting WiFi signals [1,56].

Most relevant to Wall++ are capacitive sensing methods. One of the earliest examples leveraging this phenomenon is the Theremin [18], a gesture-controlled electronic musical instrument. In HCI, researchers have frequently explored using capacitive sensing to detect the type and magnitude of body motion. For example, Mirage [45] attached electrodes to a laptop to detect dynamic poses such as arm lifting, rotating and jumping. Valtonen et al. [70] used two electrodes attached to the floor and ceiling to sense a user's height and thus can classify postures such as sitting and standing. Finally, Grosse-Puppendahl et al. [20] explored posture estimation by instrumenting furniture with multiple electrodes, for example, a couch that can detect discrete postures such as sitting and lying.

Object & Appliance Sensing
Many systems have demonstrated appliance and tool detection using cameras. For example, Snap-To-It [16] used a smartphone's camera to recognize and use appliances (e.g., an office printer). Maekawa et al. [43] utilized wrist-worn cameras to detect what object was currently being used. Finally, Zensors [34] leveraged crowd workers and machine learning to answer user-defined questions about environments, including appliances.

Another common approach is to sense sound or vibration emitted from operating appliances or objects. ViBand [36] leveraged micro-vibrations propagating through a user's
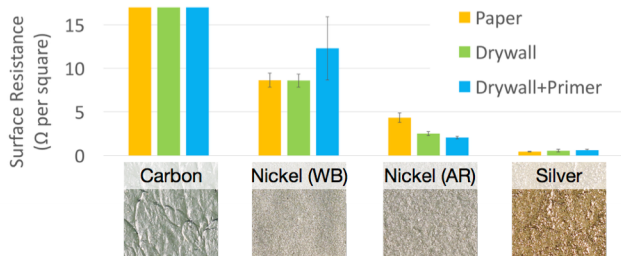
Figure 2. Conductivity test with different paints across three backing materials. Close-up of painted surface included.

Figure 3. Conductivity test with different application methods and number of coats.

body for detection. ViridiScope [31] implemented a sensor tag featuring a microphone that can infer power consumption of an appliance. Similarly, UpStream [33] attached a microphone to faucets for water consumption monitoring.

It is also possible to tag or mark an object for detection. For example, QR codes can be captured by cameras for object recognition [61]. In addition, capacitive near-field communication has been used to augment objects with antennas for communication [19]. Finally, RFID tags [38,39,67] and Bluetooth beacons (as well as most work previously reviewed on user tracking [26,32,40,46]), can also be adopted for object and appliance sensing.

Finally and closest to our sensing principle are approaches that take advantage of EM noise generated by appliances when active. This has been sensed previously by coupling to power lines [23,24,28] and users' bodies [35,71,82], or by placing sensors proximate (≤10 cm) to appliances [31,58,62,78,79]. As we will discuss, our method makes use of airborne EM signals, which enables appliance detection and tracking. We also significantly extend the sensing range beyond previous work, from centimeters to room-scale.

ELECTRODE / ANTENNA IMPLEMENTATION
The basic principle of Wall++ sensing relies on patterning large electrodes onto a wall using conductive paint. Thus, as a first step, it was necessary to develop a reliable and economically-feasible way to add large electrodes to walls. To identify suitable materials and processes, we performed a series of tests with various conductive paints, backing materials, application methods, number of coats, and topcoats. We then explored different electrode patterns suitable for our applications, and optimized them for sensing range and resolution. In all tests, we used an LCR meter to measure electrical impedance at 100 kHz.

Phase 1: Paint and Backing Materials
Both capacitive sensing and airborne EM sensing require conductive electrodes in order to induce charges freely. Thus, our first task was to identify paints that were inexpensive, non-toxic and sufficiently conductive to support our application goals. We experimented with commercially-available *carbon* [47]*, water-based nickel* [48]*, acrylic-based nickel* [49]*,* and *silver* [50] paints. Simultaneously, we tested three common backing materials: *wallpaper*, *drywall*, and *primed drywall*. All paints were applied in a single coat with a roller.
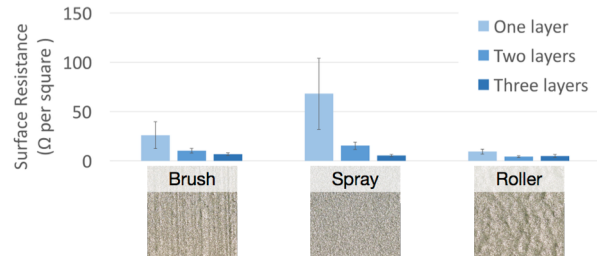
Figure 2 shows the result of this 4×3 experiment. Despite its high conductivity, we removed silver paint from consideration due to its high cost (~\$200 per m^2). Carbon paint was also eliminated due to its high resistance, which is incompatible with our technique. Among the remaining two nickel-based paints, we selected the water-based version, as it produced less odor and resulted in a smoother finish (Figure 2, bottom photos).

Phase 2: Application Method and Number of Coats
With our conductive paint selected, we next considered its application method. We varied both the number of coats and the tool used, both of which affect conductivity. We tested *brush*, *spray*, and *roller* applications with *one*, *two*, and *three* coats, resulting in a 3×3 test. Figure 3 shows these results, which consistently indicate that the surface conductivity increases with number of painted coats. Among the application methods, we selected *roller* painting, as it resulted in the highest conductivity and lower variance across the surface. As an added benefit, it was also the fastest application method.

Phase 3: Topcoat
To improve appearance and durability, we studied the effect of topcoats on our electrodes' performance. We suspected that solvents from later paint coats could interact with the conductive paint layer, affecting its conductivity. We also wanted to see if varying surface permittivity of different topcoat materials affected performance. For this experiment, we tested *no topcoat*, *acrylic*, *primer*, *latex paint* and *wallpaper*. However, we did not find any significant differences across these conditions, and thus we recommend covering Wall++ in a standard architectural latex paint for improved durability, ease of cleaning and appearance.

Phase 4: Traces & Insulation
To connect our painted electrodes, we need to run thin traces between them. Crucially, transmitter electrodes must be insulated from receiver electrodes to project most of the electric field into the air, requiring insulation between trace intersections. Thus, as a precursor to exploring electrode pattern, we first needed to identify a trace option with high conductivity and good insulation. Our tests included three materials: *copper* tape (3.2 mm width), *silver* ink drawn by pen [12] (1 mm width), and *nickel* paint applied with stencil and brush (1 mm width). Simultaneously, we tested three insulation materials: *vinyl sticker*, *latex paint* and *primer*.
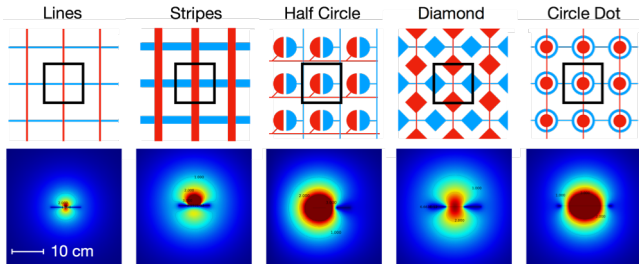
Figure 4. Top: electrode patterns we studied (transmitters in red, receivers in blue). Bottom: electric field simulations of electrodes in black region (higher voltages in red).

Conductivity test shows that copper tape had the highest conductivity (0.13 Ω/cm SD=0.0), followed by nickel paint (5.6 Ω/cm SD=4.9) and silver traces (63.5 Ω/cm SD=10.4). In the insulation test, we found that our nickel traces interacted with the latex paint and primer conditions, causing shorts, though it worked fine with vinyl stickers. Silver traces worked with all insulators, but had high variance in conductivity. Copper had the worst insulation due to a larger overlapping area, but the least variance, and for this reason, we chose it in combination with vinyl stickers (the most consistent of the insulators we tested).

Phase 5: Electrode Pattern
Having identified a reliable way to paint, connect and insulate conductive electrodes on walls, our next step was to select a pattern that enabled our desired applications. Fortunately, airborne EM sensing is not particularly sensitive to pattern geometry, and SNR is mostly of a function of antenna size. For example, previous work used copper patches [78,79] or a simple wire antenna [62]. Therefore, we chiefly optimized our design for mutual capacitive sensing, in which pattern plays a critical role. However, in Phase 7, we confirm the performance of our antenna designs in capturing airborne EM signals.

For our mutual capacitance sensing, we desired a pattern that 1) projected an electric field as far as possible, so as to provide the largest interactive volume, while also 2) offering sufficient resolution to enable fine-grained interactions, such as touch tracking. We studied five patterns common in the literature: *lines, stripes, half circle, diamond* and *circle dot* (Figure 4, top).
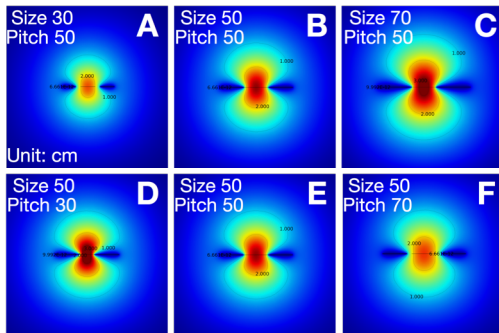

Figure 5. Simulations of diamond patterns with different sizes (A-C) and pitches (D-F).

To best evaluate the electric field projection across these designs, we ran simulations using COMSOL [13]. This provided a high-resolution view impossible to capture with hand measurements. We fixed the transmitter and receiver electrode size to 25 cm^2, except in our *lines* condition, which are purposely thin. We also fixed the distance between electrodes (i.e., pitch) to 5 cm, except in our *lines* and *stripes* conditions. We set the voltage difference between transmitters and receivers at 18 V.

Figure 4, bottom, shows our simulation results. Due to the short-range of its electric field projection, we eliminated *lines* as a candidate design. Projection range is improved with the increased electrode size in *stripes*, however there is too much inner capacitance between electrodes, which significantly reduces SNR and sensing range. The rest of the patterns do not suffer from this issue and have similar projection range. Ultimately, we selected the *diamond* pattern because it densely covers the surface, making it unlikely to miss user touches.

Phase 6: Pattern Optimization
After selecting the diamond pattern, there were two immediate parameters to tune – the size of the diamonds and the pitch. Intuitively, bigger diamonds and pitches should project larger electric fields. However, they also decrease the array's resolution. Therefore, we set out to find parameters that offered a balance between sensing range and resolution.

Figure 5, A-C, show electric field simulations at different electrode sizes (30, 50 and 70 cm) with a fixed 50 cm pitch. As expected, the bigger the electrode size, the farther the sensing range. Figure 5, D-F, show simulations at different pitches (30, 50 and 70 cm) with an electrode size fixed at 50 cm. Interestingly, bigger pitches do not improve sensing range. Combining what we discovered in this experiment, we settled on 70 cm electrodes with a 48 cm pitch – a common width of painter's tape, facilitating fabrication. As seen in Figure 6 and Video Figure, a regular *diamond* pattern can be efficiently produced by laying down a cross-hatch of painter's tape, and then using a paint roller.

Phase 7: Antenna Sensitivity
Phases 5 and 6 were primarily focused on mutual capacitance sensing. In this design phase, we wished to verify that our selected diamond pattern could robustly capture airborne EM signals. There are many ways to configure diamond patterns into an antenna array. For example, we could connect all columns and rows together to make one large antenna. However, this monolithic antenna eliminates the possibility of triangulating signal sources, discussed later.

Therefore, we investigated the idea of selecting a subset of diamond columns as antennas (as illustrated in Figure 1F). These need not be single columns, but could be several adjacent columns connected together. To see if this improved signal, we conducted a test in a shielded chamber with minimal EM noise. To be able to vary antenna size, we painted diamond electrode patterns on individual 1×8' foam boards,
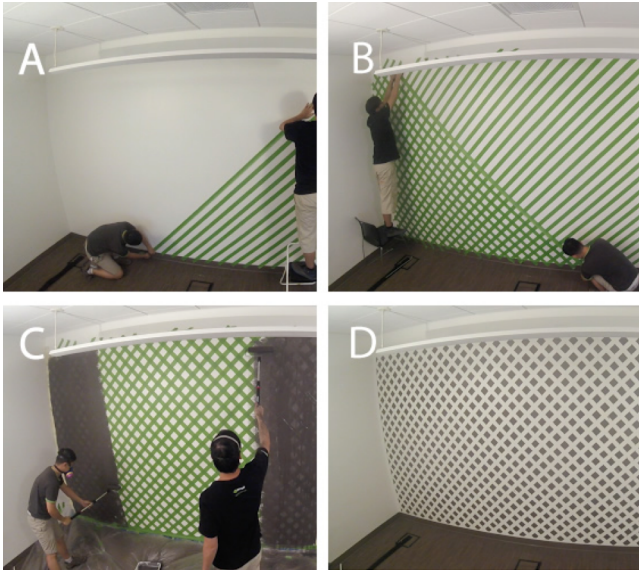
Figure 6. Painter's tape is laid down in a crosshatched pattern (A & B), and then painted en masse with e.g., a roller (C) to create a grid of regular diamonds (D).

each of which acted as a single-column antenna, but which could be connected together to make a multi-column antenna. We varied the number of columns in the antenna unit from 1 to 3, with a known signal source placed 50 cm away.

Result indicated that larger antenna sizes offered improved signal strength. However, the improvement was minor – a three-columned-antenna only improved signal strength by 15% over a single column unit. Given the gain was modest, we decided to use single column antennas for circuit simplicity and improved spatial resolution.

Next, to better quantify the sensitivity of single-column antennas, we collected EM signals from 12 appliances at varying distances. As can be seen in Figure 7, all of our test appliances can be sensed within a 2-meter range, and some noisy devices up to 4 meters. We also found serendipitously that the human body broadcasts EM signals when holding and operating some appliances. For example, a hairdryer we tested had no visible signal unless a user was grasping it. We also found a class of appliances that only activate when touched (chiefly for power conservation), e.g., laptop track-
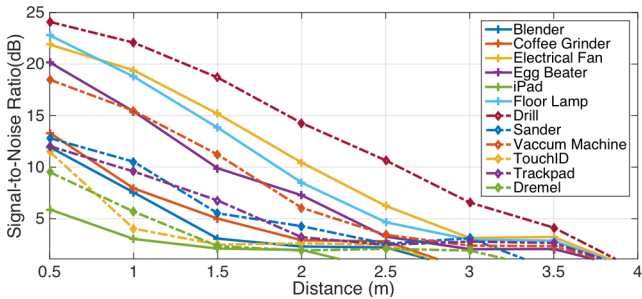

Figure 7. Received signal strength collected with appliances operating at different distances to the wall antenna.

pads and smartphone fingerprint readers. However, this has the interesting potential to allow for recognition of human activities at the moment of user engagement.

Phase 8: Wall Construction
After we finalized our fabrication parameters, we painted a real wall at our institution, measuring 12×8' (3.7×2.4 m), seen in Figure 1 (B & D) and Figure 6. We used this wall to verify our previous focused experiments. This wall has 22 columns and 15 rows of electrodes, for a total of 37 coaxial cable connections to our custom sensing hardware. After we *nickel* painted the wall with a *diamond* pattern, we finished it with a standard latex paint. In total, the wall took roughly four hours to complete with a total material cost under $200. We anticipate that the time and material cost of a commercially-deployed solution would be significantly reduced with trained painters and bulk material purchase. A time lapse of this painting process is documented in our Video Figure.

SENSING HARDWARE IMPLEMENTATION
To enable user and environment sensing, Wall++ employs two distinct sensing modes: mutual capacitive sensing and airborne EM sensing. This required development of custom sensor boards (Figure 8), built around a Cortex M4 microcontroller running at 96 MHz (MK20DX256VLH7 [15]), powered by Teensy 3.2 firmware [55]. Our main board (Figure 8A) plugs into two multiplexing boards, one designed for mutual capacitance sensing (Figure 8B) and another for EM sensing (Figure 8C). In the future, these could be integrated into a compact, single-board design.

Mutual Capacitance Sensing
To detect a user's hands and body pose, we use mutual capacitance sensing, which measures the capacitance between two electrodes [6,8]. This sensing technique is the basis of modern touchscreens as seen in smartphones and tablets. When a body part is near a transmitter-receiver pair, it interferes with the projected electric field, reducing the received current, which can be measured. This is referred to as shunting mode [65,66,83] sensing. On the other hand, if the user's body directly touches an electrode, it greatly increases the capacitance and received current. See [21] for a more thorough review of capacitive sensing in HCI.

In capacitive sensing mode, our main board uses an AD5930 [3] DDS to generate a 100 kHz sine wave as the excitation signal. This signal is amplified to 18 V peak-to-peak by the multiplexing board (Figure 8B) and routed to a specified transmitter electrode column (Figure 1A, red). We use another set of multiplexers to connect a receiver electrode row (Figure 1A, blue) to our analog frontend, which is filtered and amplified. We use an AD637 RMS-DC converter [4] to measure the amplitude of the received signal, which correlates to the capacitance between the current transmitter and receiver electrodes. We set the integration time for the AD637 to 100 microseconds (i.e., 10 periods of the excitation signal). The output of the converter is sampled by our microcontroller's built-in ADC.
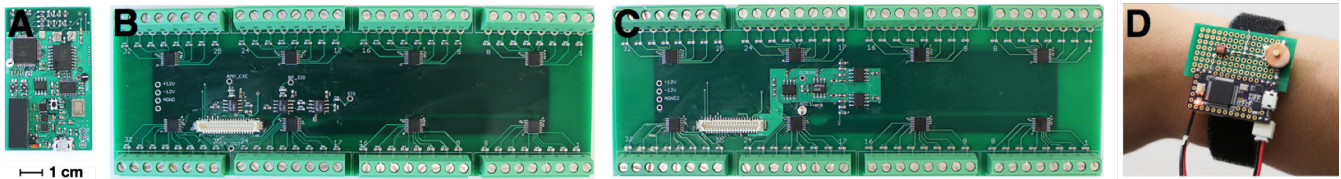
Figure 8. Different hardware components we developed. A) Main sensor board, B) capacitive sensing multiplexing board, C) EM multiplexing board, and D) signal-emitting wristband. Uniform scale.

Our 12×8' augmented wall has 22 columns and 15 rows. At any moment, only one transmitting column and one receiving row are selected for mutual capacitance sensing. The circuit measures the mutual capacitance between the two electrodes, which is most strongly affected by a user's body being proximate to (or touching) the intersection of the column and row. The circuit then moves on to the next row-column pair until all 22×15 = 330 measurements are collected. These measurements are then sent to a laptop over USB at 16.5 FPS.

Airborne EM Sensing

In EM sensing mode, no active signals are injected into the wall's electrodes. The multiplexing board (Figure 8C) features a differential amplification circuit with a 159 Hz high pass filter to remove DC components and powerline noise. One terminal of the input is connected to common ground, while the other terminal is cycled through columns, one at a time, each serving as a signal-column antenna. The signal is then amplified with a gain value of 100 and DC biased to AVDD/2 (1.65V) before sampling.

Our microcontroller's two built-in ADCs are configured into a high-speed, interleaved DMA mode, enabling a sampling rate of 4 MHz with 12-bit resolution. We collect 1024 ADC measurements and perform an on-board FFT computation. To better capture transient EM spikes, the board performs this measurement 20 times, and records the maximum value for each FFT bin as the result. This process takes ~20 milliseconds per column, resulting in an FPS of 6.2 for an 8-column-attenna setup.

TOUCH SENSING

Mutual capacitive sensing enables Wall++ to track a user's hand hovering above or touching a wall's surface. We first describe our software implementation, followed by our evaluation procedure and results.

Software

Due to fabrication inconsistencies, the raw capacitance measured at each row-column pair can vary. To compensate for this, we capture a background profile and convert all measurements into *z*-scores. When a user touches the wall, a transmitter and receiver pair are capacitively shorted, which makes the touched region have a significantly higher capacitance than the captured background. We can visualize this as a pixel in a capacitive image (Figure 1C), which is thresholded to get touch coordinates. When a user's hand is hovering above a wall, it capacitively couples to many row-column pairs, appearing as a negative blob in the capacitive

image. For hover tracking, we identify blobs of activated pixels, and interpolate the peak by calculating the center of mass in a 3×3 pixel area.

Evaluation

To investigate the hand tracking performance of Wall++, we recruited 14 participants (7 female, average age of 24). The heights of these participants ranged from 160 to 183 cm, with masses ranging from 50 to 90 kg. The study took roughly 40 minutes to complete and participants were compensated $20 for their time. We used our 12×8' wall as the test apparatus. A calibrated projector was used to render experimental prompts for participants. Additionally, a small plastic-runged ladder was provided if requested points were beyond a participant's reach (which also provided a more challenging grounding condition to study).

We first asked participants to walk around for 10 minutes roughly one meter away from the wall. This provided 9900 *no user present* trials per participant. We then asked participants to "click" points digitally projected onto the wall's surface. When a point turned red, participants placed their hand to that point, allowing for 30 *touch* coordinates to be recorded over a 2 second period. The point then turned green, at which point participants held their hands roughly 10 cm from the point; 30 *hover* coordinates were recorded. No feedback about the tracking result was shown to participants. In total, 50 fully randomized points were requested from each of our 14 participants, resulting in 21,000 *touch* and 21,000 *hover* trials.

Results

Of the 138,600 *no user present* data points, representing 140 minutes of data, there were no touch or hover events reported by our system (i.e., 100% accuracy). Of our 21,000 *touch* trials, 97.7% (SD=2.4) were correctly labeled as touch events by our system (2.3% were incorrectly detected as hovers). *Hover* detection was 99.8% (SD=0.3) accurate.
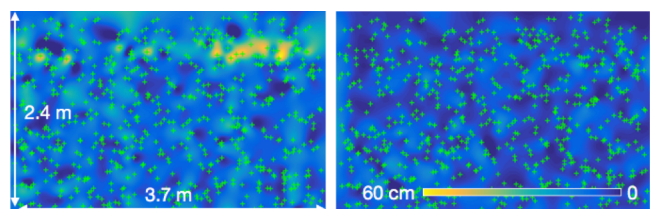

Figure 9. Touch (left) and hover (right) tracking distance error on our test wall (interpolated across surface). Green crosshairs show (50×14) 700 requested locations.
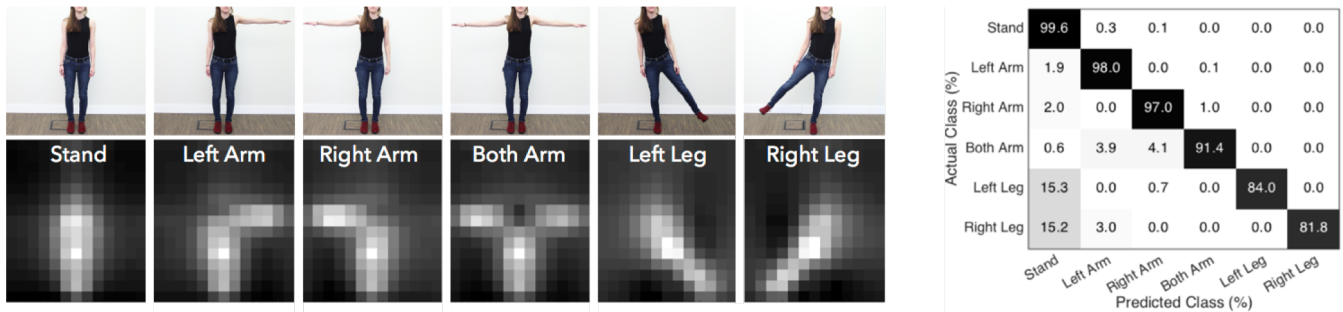
Figure 10. Left: six poses (top) and averaged capacitive images from the user study (bottom). Right: confusion matrix for 6 poses.

Using requested coordinates and our system's reported coordinates, we calculated the Euclidian distance error for our touch and hover trials. We found a mean *touch* tracking distance error of 13.7 cm (SD=1.1) and a mean *hover* tracking distance error of 6.5 cm (SD=0.3). Figure 9 provides an interpolated error heat map across our wall's surface. There is one region of reduced accuracy, which we suspect is due to either a fabrication defect or possibly metal/electrical infrastructure behind the wall. Also, we did not see any reduction in accuracy for participants who used the ladder for reaching high points.

POSE ESTIMATION

Wall++ can also estimate body pose of users if they are close to a wall. We now describe this software implementation, evaluation procedure and study results.

Software

As with touch and hover tracking, pose estimation uses a *z*-scored capacitive image as input. We first look for users by sliding a 3×15 window along the x-axis, searching for a blob of sufficient total activation. If a region is found to be above threshold, pose estimation is triggered for that bounding box. Along the center column, pixels above a second threshold are labeled as the torso. We then scan to the left and right of the blob, labeling bottom extents as feet and upper extents as hands. An example of these five key points is shown in Figure 1, D and E. We can use these key points to characterize different body poses; for evaluation, we included *standing, left arm* lifted*, right arm* lifted*, both arms* lifted*, left leg* lifted*,* and *right leg* lifted (Figure 10).

Evaluation

We used the same group of participants and apparatus as our touch tracking study. In total, there were five rounds of live testing. At the beginning of each round, we assigned participants to a random standing location 20 cm in front of the wall. They were then asked to perform the six test poses, sequentially, and in a random order. For each pose, we recorded 30 data points over a 2 second period, which resulted in 12,600 pose trials (5 rounds × 6 poses × 30 trials × 14 participants).

Results

Of the 12,600 trials we captured, 99.8% (SD=0.6) triggered our pose estimation pipeline. Overall, the system inferred the correct pose in 92.0% (SD=3.5) of trials; a confusion matrix is provided in Figure 10. The greatest source of error (63.5%) is from *left leg* and *right leg* being confused with *stand*. Figure 10, bottom-left, shows the averaged capacitive image for each pose (all trials and participants combined). We also found the torso key point accurately reflected a user's location along the wall, with a mean distance error of 8.6 cm (SD=2.2).

APPLIANCE DETECTION

Wall++ captures airborne EM signals emitted by electrical appliances when running. In this section, we focus on detecting the on/off state of appliances (i.e., detection, but not localization). In being a room-scale sensing technique, Wall++ had to solve two important challenges, which differentiates us from prior work. First, unlike EM sensing with conductive media (e.g., powerlines [23,24,28], human bodies [35,71,82]), air substantially attenuates EM signals, which would generally preclude long-range airborne EM sensing. We overcome this by using large antennas. Second, unlike worn EM detectors [35], which can generally assume that only one appliance is grasped at any given time, Wall++ must handle simultaneous active appliances. For this, we use a special pipeline, described next.

Software

To help suppress persistently noisy EM bands (from e.g., florescent light ballasts), our system computes and uses *z*-scored FFTs. Before appliances can be recognized, they must be registered in our system. This is done by capturing data while an appliance is active, and recording its FFT signature. We then threshold this FFT to create a bitmask representing characteristic frequencies for that appliance.

When live data is being streamed from our sensor board, the incoming FFTs are bit-masked against each known appliance and passed to a corresponding, appliance-specific SMO classifier (Poly Kernel, E=1.0 [25]. Output: *running* or *not running*). In essence, this bit-masking approach has the effect of making each appliance classifier blind to non-relevant EM bands, which enables multi-appliance detection, reduces training data collection, and improves overall robustness. We used a one-second classification hysteresis to reduce spurious appliance detections. The result of this process is a list of active appliances detected at each antenna. These sets are unioned to provide a list of active appliances in the room.
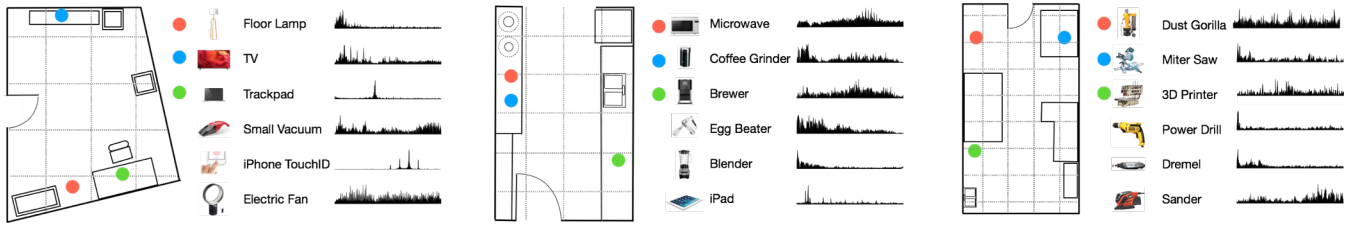
**Figure 11. On the left: floor plans of an office (left), kitchen (center), and workshop (right).
On the right: appliances and their EM profiles (0 to 2 MHz). One-meter-spaced grids are shown in dashed lines.**

Evaluation

Room-scale appliance detection requires all walls to be augmented. However, our previous test apparatus was only a single wall (12×8'). To simulate a fully augmented room, we distributed 1×8' column antennas we had previously made for our Antenna Sensitivity study. As an added benefit, this apparatus allowed us to run our experiment in three different locations: office, kitchen, and workshop (Figure 11). At each location, we evenly distributed eight column antennas around the room periphery, working around windows and doorways as needed.

In each location, we tested six contextually-appropriate appliances: three fixed and three mobile. The locations of fixed appliances are color coded in Figure 11, while we randomized the position of mobile appliances according to a one-meter grid we laid out in each room. We omitted locations blocked by furniture, resulting in 12 test points in the *Office,* 14 in the *Kitchen*, and 26 in the *Workshop.*

To train our system for a room and its appliances, we collected EM signals using one antenna. In total, there were three rounds of training data collection. In each round, 90 data points were recorded over 15 seconds when no appliance was active. We then collected 90 data points for each appliance while active (one at a time), during which we varied the distance between the appliance and the antenna up to 2 meters. We then trained a classifier for each appliance, using the background data (i.e., no appliance running) and the other five appliances as negative examples.

At each location, we performed three rounds of live testing at different times of day – morning (~8 am), noon (~12 pm), and late night (~11 pm) – when the building had different environmental conditions, occupancy load, etc. In each round of testing, we first recorded 10 minutes of data (3720 data points) when no appliances were active, to test for false positives resulting from background EM noise. We then activated all six appliances, one at a time, in a random order. As an added experiment, we also turned on all three fixed appliances simultaneously. In all trials, we turned on and off the appliances five times each. Real-time detection results were recorded.

Results

Across the 90 minutes (33,480 data points) of data collected when no appliance was turned on, 1.3% (SD=1.0) of trials were labelled as having an appliance running (i.e., false positives). Across all trials when appliances were running, 85.3% (SD=4.9) correctly classified the active appliances. We found that mobile appliances contributed 88.4% (SD=12.8) of the errors, mostly when they were at the center of rooms and far from any antenna.

We found no significant difference in accuracy across time of day. However, we did found that background noise changed over time, and thus we had to recapture the background profile for our *z*-score computation at the start of each session. This indicates that Wall++ will need a dynamic backgrounding scheme when deployed.

APPLIANCE LOCALIZATION

Airborne EM signals attenuate as they radiate in air, leading to different signal amplitudes across a distributed array of antennas, such as column antennas along the walls of a room. Wall++ leverages this affect to localize the source of EM signals, and even track the source if mobile. In this section, we describe our tracking pipeline, and its evaluation and results.

Software

Our tracking pipeline extends our Appliance Detection pipeline by additionally using the masked FFTs to calculate a received signal strength (RSS) as P_i in (1) for each known appliance at each antenna. According to the Friis transmission formula [17], the relation between the appliance's location and its RSS measured at the *i*-th antenna can be modelled as

$$f_i(x, y, A_T): \frac{A_T G_i}{(x-x_i)^2+(y-y_i)^2} = P_i \quad (1)$$

Here, P_i is the received signal strength at the *i*-th antenna, G_i is the sensitivity of antenna i, (x_i, y_i) are the coordinates of the *i*-th antenna, and A_T is the transmitter's radiated power. Therefore, an appliance's location can be obtained by solving an L2-norm minimization problem:

$$\min_{x,y,A_T} \sum_{i=1}^{L} \|f_i(x, y, A_T) - P_i\|_2 \quad (2)$$

We first calibrated our system using a known, single-tone transmitter to estimate G_i for the i-th antenna. Then, we used the Nelder-Mead optimization method from the Python scipy package [64] to minimize eq. (2).

Given a received signal P_i at *i*-th antenna with its respective location x_i, y_i and the sensitivity G_i, equation (2) can return both the unknown appliance location (x, y) and its radiated power A_T. Although different appliances have different

radiated power, our algorithm does not depend on prior knowledge of an appliance's absolute radiated power A_T, as the computation is relative. Since we have three unknown parameters (x, y, A_T) in (2), at least $L \geq 3$ column antennas are needed to produce a location estimate. Intuitively, the more antennas, the more data the algorithm can use for convergence, improving localization accuracy.

Evaluation
For this evaluation, we used the same mobile appliances, rooms, and column antenna deployment as our Appliance Detection study (Figure 11). For each room, we collected 40 data points (over ~6 seconds) for three mobile appliances at all points on our one-meter grids (which acted as a spatial ground truth). As before, we omitted grid points blocked by furniture. In total, 6,240 data points (12+14+26 grid locations × 40 data points × 3 appliances) were collected for analysis.

Results
Our tracking algorithm localized appliances with a mean distance error of 1.4 m (SD=0.5). Figure 12 (top) illustrates this error across our one-meter room grids. As can be seen, accuracy varies considerably even in a single room (e.g., workshop – Figure 12, top-right – best tracking accuracy: 0.6 m; worst: 3.6 m), but overall suggests feasibility.

We also considered deployment in real-world locations where doors, windows and other infrastructure might block the placement of Wall++. To simulate this, and investigate how much it affects localization accuracy, we ran a post hoc study removing an increasing number of antennas from the room (Figure 13). More specifically, for each antenna count, we randomly selected a subset of antennas and reran our localization algorithm using only those data. We repeated this random selection three times for each antenna count and averaged the results.

As expected, tracking error increases as fewer antennas are available. However, even in the worst-case scenario, with only three antennas, we can still localize appliances to within 4 meters on average, which is coarse, but still potentially useful. It also appears likely that using more than 8 antennas would yield even better tracking accuracies. This would be the case in a fully realized installation of Wall++, as our recommend pattern has 8 column attenas every 1.35 m (Figure 6); a 4×4 m room would have roughly 100 antennas.

USER TRACKING & IDENTIFICATION
We have already discussed how Wall++ can track appliances when they are radiating EM signals. This motivated us to build a small, signal-emitting wristband (Figure 8D) to enable user localization and identification using the same physical setup and tracking pipeline as appliances.

Our signal-emitting wristband uses a Teensy microcontroller attached to an LC tank, driven by a 3.3 V PWM signal set at a frequency between 800 kHz and 3 MHz. By enabling/disabling the drive pin, the emitted signal can be turned on or off, creating an on-off-keying (OOK) signal that we use to communicate with Wall++ (Figure 1, I & J) at a maximum speed of 300 baud. Though the throughput is low, it is more than sufficient to transmit a user ID, and even low-speed sensor data, such as heartrate. Figure 1J shows a waterfall spectrogram from 1.4 to 1.6 MHz with a 1.5 MHz carrier frequency (seen as red line segments).

Evaluation
To evaluate Wall++ for *user tracking*, we conducted an evaluation using a similar procedure to our Appliance Localization study. We configured the wristband to emit a constant 1.5 MHz signal. In each of our three rooms, we asked 5 participants to wear our wristband, and stand on the one-meter grid points sequentially, during which we collected 40 data points (~6 seconds). As before, we omitted grid points that were blocked by furniture.

We also ran a basic study to investigate the *data transmission performance* over different distances between a participant and a wall antenna. For this test, we used one column antenna sampled at 120 FPS. As a proof-of-concept evaluation, we configured our wristband to output at 20 bits/sec, transmitting a 6-bit header, 8-bit payload length, 16-bit user ID, and 5-bit tail (35 bits in total; Figure 1J). We recruited 5 participants to wear our wristband, and asked them to stand 1, 2, 3 and 4 meters away from the antenna. At each distance, we recorded 5 data transmissions from the wristband.

Results
Our *user tracking* results show an average distance error of 1.4 m (SD=0.6). This performance is almost identical to our

Figure 12. Tracking distance error at our three test locations. Left to right: office, kitchen and workshop.
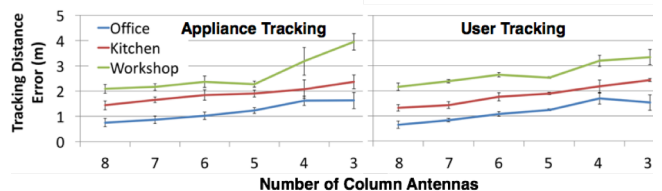

Figure 13. Tracking distance error using different numbers of column antennas (three locations tested).

Appliance Localization results. Figure 12, bottom, illustrates the tracking error across each room. We also ran a post hoc study to investigate how the number of antennas in a room would affect tracking accuracy (see counterpart study in Appliance Localization for procedure). As before, accuracy decreases with antenna count (Figure 13), but coarse tracking remains feasible with just three antennas.

With respect to *data transmission performance*, there were no bit errors for all trials collected within 3 meters of the antenna. However, at 4 meters, the bit error rate increased to 46.4% (SD=26.3). This was due to the carrier signal getting subsumed into background noise. Nonetheless, a 3-meter range would be sufficient for all three of our tested locations (i.e., no point is greater than 3 meters from wall). It is also likely that longer communication range can be achieved by using a higher amplitude emitted signal, or by applying standard error correction techniques.

EXAMPLE USES

Touch sensing, pose tracking, and activity detection are well trodden ground in HCI. Additionally, Wall++ can work in concert with many existing feedback mechanisms, including screens (e.g., TVs, smart appliances, wearables), voice interfaces (e.g., Google Home, Amazon Echo) and ambient displays (e.g., smart light bulbs). We offer some illustrative example uses:

Touch Tracking, for example, could enable flexible-placement of wall-borne buttons to e.g., turn on/off lights, or provide a number keypad to unlock a door. Wall++'s continuous touch tracking could allow slider-like input to adjust e.g., light level, room temperature, or music volume; discrete swipes could be used to change lighting mode, or move between songs.

Pose Tracking could allow users to play video games with their backs near to a wall and control avatars on a TV across the room. Pose tracking could also be useful in inferring human activity and context when users are near to work surfaces, e.g., making dinner vs. coffee on a kitchen countertop. Desks are often pushed up against walls, where Wall++ can detect the presence of a user's legs for occupancy tracking. In narrow hallways, we can track users' locomotion (e.g., direction, speed, gait), perhaps even identifying occupants.

Activity Recognition is made possible by Wall++'s ability to detect appliance operation, and then track that appliance in a room (and potentially a whole building). This rich source of contextual information can directly inform smart environments and assistive virtual agents. For example, a room can automatically adjust its lighting and window blinds when Wall++ detects a TV waking from standby. Users could also subscribe to alerts when certain appliances turn off, such as a laundry machine or electric kettle.

LIMITATIONS

Cost. Since walls are pervasive and expansive, the cost of any wall treatment to enable Wall++ needs be low in order to be plausible. Our recommended materials and antenna pattern cost $21.30 per m^2 for the small number of walls that we augmented for this project. While significantly less expensive than conventional touchscreen technologies, it is still expensive for e.g., a home (which might have 100 m^2 of walls). We believe replacing copper tape with conductive paint traces, as well as purchasing materials in bulk, could significantly reduce cost.

Installation Complexity. Although Wall++ does not require any special materials or equipment, it still requires a fair amount of wiring effort, as each row and column needs to be connected to a sensor board, presumably hidden in or behind the wall. We also found that applying paint evenly is challenging – our "final" 12×8' wall still showed some fabrication variance, as seen Figure 9. While within the capabilities of a home DIY enthusiast, it is probably beyond the skill and comfort level of the average consumer.

Interference. Environmental EM noise from e.g., fluorescent lights, can affect Wall++. This is a minor issue in active mutual capacitance sensing, as our excitation signal dominates the received signal. However, in passive EM sensing mode, environmental noise can have a significant impact on SNR. Among our three tested locations, *workshop* had the noisiest EM environment, which no doubt contributed to it having the lowest accuracies.

Nearby Grounded Objects. We found that well-grounded objects near to a wall, such as a TV, attenuates the shunting effect of a user's body, which in turn interferes with our mutual capacitance sensing. We found a similar effect with airborne EM signals. This finding suggests that real-world installations should avoid using (i.e., skip or disable) antennas that are proximate to such objects. This issue might also be mitigated by using a superior background calibration process and an analog frontend with a programmable gain.

Sensing Range. Our implementation of body pose and airborne EM sensing have limited sensing range (roughly 0.5 and 3 meters respectively). Fortunately, for appliance detection and localization, we found that most appliances in real world settings are close to walls, chiefly because electrical power is provided along the walls (and not in the middle of rooms). While there are some inherent sensing limitations, we do believe that range can be increased with superior circuit topology and software improvements in the future.

CONCLUSION

In this work, we introduced Wall++, a low-cost sensing technique that can turn ordinary walls into smart infrastructure, able to sense interactions and activities happening in a room, and potentially throughout an entire building. Our multi-phase exploration of materials, application methods, and electrode patterns informed our proof-of-concept hardware and software implementation. Then, through a series of user studies, we demonstrated that Wall++ can robustly track user touches and poses, as well as detect and track appliances (or tagged users) in a room.

REFERENCES
1. Fadel Adib, Chen-Yu Hsu, Hongzi Mao, Dina Katabi, and Frédo Durand. 2015. Capturing the human figure through a wall. ACM Trans. Graph. 34, 6, Article 219 (October 2015), 13 pages. DOI: https://doi.org/10.1145/2816795.2818072

2. Ramezani Akhmareh, Alireza, Mihai Teodor Lazarescu, Osama Bin Tariq, and Luciano Lavagno. "A Tagless Indoor Localization System Based on Capacitive Sensing Technology." Sensors 16, no. 9 (2016): 1448. DOI: https://doi.org/10.3390/s16091448.

3. Analog Devices. Datasheet. Retrieved September 18, 2017 from http://www.analog.com/media/en/technical-documentation/data-sheets/AD5930.pdf

4. Analog Devices. Datasheet. Retrieved September 18, 2017 from http://www.analog.com/media/en/technical-documentation/data-sheets/AD637.pdf

5. Thomas Augsten, Konstantin Kaefer, René Meusel, Caroline Fetzer, Dorian Kanitz, Thomas Stoff, Torsten Becker, Christian Holz, and Patrick Baudisch. 2010. Multitoe: high-precision interaction with back-projected floors based on high-resolution multi-touch input. In Proceedings of the 23nd annual ACM symposium on User interface software and technology (UIST '10). ACM, New York, NY, USA, 209-218. DOI: https://doi.org/10.1145/1866029.1866064

6. Gary Barrett, and Ryomei Omote. "Projected-capacitive touch technology." Information Display 26, no. 3 (2010): 16-21.

7. Hrvoje Benko, Andrew D. Wilson, and Federico Zannier. 2014. Dyadic projected spatial augmented reality. In Proceedings of the 27th annual ACM symposium on User interface software and technology (UIST '14). ACM, New York, NY, USA, 645-655. DOI: https://doi.org/10.1145/2642918.2647402

8. Larry K. Baxter "Capacitive sensors." Ann Arbor 1001 (2000): 48109.

9. Alan Bränzel, Christian Holz, Daniel Hoffmann, Dominik Schmidt, Marius Knaust, Patrick Lühne, René Meusel, Stephan Richter, and Patrick Baudisch. 2013. GravitySpace: tracking users and their poses in a smart room using a pressure-sensing floor. In Proceedings of the SIGCHI Conference on Human Factors in Computing Systems (CHI '13). ACM, New York, NY, USA, 725-734. DOI: https://doi.org/10.1145/2470654.2470757

10. Andreas Braun, Sebastian Zander-Walz, Stefan Krepp, Silvia Rus, Reiner Wichert, and Arjan Kuijper. 2016. CapTap: combining capacitive gesture recognition and acoustic touch detection. In Proceedings of the 3rd International Workshop on Sensor-based Activity Recognition and Interaction (iWOAR '16). ACM, New York, NY, USA, Article 6, 6 pages. DOI: https://doi.org/10.1145/2948963.2948969

11. Zhe Cao, Tomas Simon, Shih-En Wei, and Yaser Sheikh. "Realtime multi-person 2d pose estimation using part affinity fields." arXiv preprint arXiv:1611.08050 (2016).

12. Circuit Scribe. Product Information. Retrieved September 18, 2017 from https://www.circuitscribe.com/product/circuit-scribe-pen-single/

13. COMSOL multiphysics user's guide. Version: September 10 (2005): 333.

14. Gabriel Deak, Kevin Curran, and Joan Condell. 2012. Review: A survey of active and passive indoor localization systems. Comput. Commun. 35, 16 (September 2012), 1939-1954. DOI: http://dx.doi.org/10.1016/j.comcom.2012.06.004

15. Freescale Semiconductor. Datasheet. Retrieved September 18, 2017 from http://cache.freescale.com/files/32bit/doc/data_sheet/K20P64M72SF1.pdf

16. Adrian A. de Freitas, Michael Nebeling, Xiang 'Anthony' Chen, Junrui Yang, Akshaye Shreenithi Kirupa Karthikeyan Ranithangam, and Anind K. Dey. 2016. Snap-To-It: A User-Inspired Platform for Opportunistic Device Interactions. In Proceedings of the 2016 CHI Conference on Human Factors in Computing Systems (CHI '16). ACM, New York, NY, USA, 5909-5920. DOI: https://doi.org/10.1145/2858036.2858177

17. Harald. T. Friis, "A Note on a Simple Transmission Formula" in Proceedings of the IRE, vol. 34, no. 5, pp. 254-256, May 1946. DOI: https://doi.org/10.1109/JRPROC.1946.234568

18. Albert Glinsky. 2000. Theremin: Ether Music and Espionage. University of Illinois Press. http://books.google.de/books?id=6DHlQJcMpBQC

19. Tobias Grosse-Puppendahl, Sebastian Herber, Raphael Wimmer, Frank Englert, Sebastian Beck, Julian von Wilmsdorff, Reiner Wichert, and Arjan Kuijper. 2014. Capacitive near-field communication for ubiquitous interaction and perception. In Proceedings of the 2014 ACM International Joint Conference on Pervasive and Ubiquitous Computing (UbiComp '14). ACM, New York, NY, USA, 231-242. DOI: https://doi.org/10.1145/2632048.2632053

20. Tobias Grosse-Puppendahl, Alexander Marinc, and Andreas Braun. 2011. Classification of user poses with capacitive proximity sensors in AAL-Environments. In Proceedings of the Second international conference on Ambient Intelligence (AmI'11). Springer-Verlag, Berlin, Heidelberg, 314-323. DOI: http://dx.doi.org/10.1007/978-3-642-25167-2_43

21. Tobias Grosse-Puppendahl, Christian Holz, Gabe Cohn, Raphael Wimmer, Oskar Bechtold, Steve Hodges, Matthew S. Reynolds, and Joshua R. Smith. 2017. Finding Common Ground: A Survey of Capacitive Sensing in Human-Computer Interaction. In Proceedings of the 2017 CHI Conference on Human Factors in Computing Systems (CHI '17). ACM, New York, NY, USA, 3293-3315. DOI: https://doi.org/10.1145/3025453.3025808

22. Nan-Wei Gong, Steve Hodges, and Joseph A. Paradiso. 2011. Leveraging conductive inkjet technology to build a scalable and versatile surface for ubiquitous sensing. In Proceedings of the 13th international conference on Ubiquitous computing (UbiComp '11). ACM, New York, NY, USA, 45-54. DOI: https://doi.org/10.1145/2030112.2030120

23. Manoj Gulati, Shobha Sundar Ram, and Amarjeet Singh. 2014. An in depth study into using EMI signatures for appliance identification. In Proceedings of the 1st ACM Conference on Embedded Systems for Energy-Efficient Buildings (BuildSys '14). ACM, New York, NY, USA, 70-79. DOI: http://dx.doi.org/10.1145/2674061.2674070

24. Sidhant Gupta, Matthew S. Reynolds, and Shwetak N. Patel. 2010. ElectriSense: single-point sensing using EMI for electrical event detection and classification in the home. In Proceedings of the 12th ACM international conference on Ubiquitous computing (UbiComp '10). ACM, New York, NY, USA, 139-148. DOI: http://dx.doi.org/10.1145/1864349.1864375

25. Mark Hall, Eibe Frank, Geoffrey Holmes, Bernhard Pfahringer, Peter Reutemann, and Ian H. Witten. 2009. The WEKA data mining software: an update. SIGKDD Explor. Newsl. 11, 1 (November 2009), 10-18. DOI: http://dx.doi.org/10.1145/1656274.1656278

26. Josef Hallberg, Marcus Nilsson, and Kåre Synnes. "Positioning with bluetooth." In Telecommunications, 2003. ICT 2003. 10th International Conference on, vol. 2, pp. 954-958. IEEE, 2003. DOI: http://dx.doi.org/10.1109/ICTEL.2003.1191568

27. Chris Harrison and Scott E. Hudson. 2008. Scratch input: creating large, inexpensive, unpowered and mobile finger input surfaces. In Proceedings of the 21st annual ACM symposium on User interface software and technology (UIST '08). ACM, New York, NY, USA, 205-208. DOI: https://doi.org/10.1145/1449715.1449747

28. George Hart. "Nonintrusive appliance load monitoring." Proceedings of the IEEE 80, no. 12 (1992): 1870-1891. DOI: http://doi.org/10.1109/5.192069

29. Hiroshi Ishii, Craig Wisneski, Julian Orbanes, Ben Chun, and Joe Paradiso. 1999. PingPongPlus: design of an athletic-tangible interface for computer-supported cooperative play. In Proceedings of the SIGCHI conference on Human Factors in Computing Systems (CHI '99). ACM, New York, NY, USA, 394-401. DOI: http://dx.doi.org/10.1145/302979.303115

30. Brett Jones, Rajinder Sodhi, Michael Murdock, Ravish Mehra, Hrvoje Benko, Andrew Wilson, Eyal Ofek, Blair MacIntyre, Nikunj Raghuvanshi, and Lior Shapira. 2014. RoomAlive: magical experiences enabled by scalable, adaptive projector-camera units. In Proceedings of the 27th annual ACM symposium on User interface software and technology (UIST '14). ACM, New York, NY, USA, 637-644. DOI: https://doi.org/10.1145/2642918.2647383

31. Younghun Kim, Thomas Schmid, Zainul M. Charbiwala, and Mani B. Srivastava. 2009. ViridiScope: design and implementation of a fine grained power monitoring system for homes. In Proceedings of the 11th international conference on Ubiquitous computing (UbiComp '09). ACM, New York, NY, USA, 245-254. DOI: http://dx.doi.org/10.1145/1620545.1620582

32. Antti Kotanen, Marko Hannikainen, Helena Leppakoski, and Timo D. Hamalainen. "Experiments on local positioning with Bluetooth." In Information Technology: Coding and Computing [Computers and Communications], 2003. Proceedings. ITCC 2003. International Conference on, pp. 297-303. IEEE, 2003. DOI: https://doi.org/10.1109/ITCC.2003.1197544

33. Stacey Kuznetsov and Eric Paulos. 2010. UpStream: motivating water conservation with low-cost water flow sensing and persuasive displays. In Proceedings of the SIGCHI Conference on Human Factors in Computing Systems (CHI '10). ACM, New York, NY, USA, 1851-1860. DOI: https://doi.org/10.1145/1753326.1753604

34. Gierad Laput, Walter S. Lasecki, Jason Wiese, Robert Xiao, Jeffrey P. Bigham, and Chris Harrison. 2015. Zensors: Adaptive, Rapidly Deployable, Human-Intelligent Sensor Feeds. In Proceedings of the 33rd Annual ACM Conference on Human Factors in Computing Systems (CHI '15). ACM, New York, NY, USA, 1935-1944. DOI: https://doi.org/10.1145/2702123.2702416

35. Gierad Laput, Chouchang Yang, Robert Xiao, Alanson Sample, and Chris Harrison. 2015. EM-Sense: Touch Recognition of Uninstrumented, Electrical and Electromechanical Objects. In Proceedings of the 28th Annual ACM Symposium on User Interface Software & Technology (UIST '15). ACM, New York, NY, USA, 157-166. DOI: https://doi.org/10.1145/2807442.2807481

36. Gierad Laput, Robert Xiao, and Chris Harrison. 2016. ViBand: High-Fidelity Bio-Acoustic Sensing Using Commodity Smartwatch Accelerometers. In Proceedings of the 29th Annual Symposium on User Interface Software and Technology (UIST '16). ACM, New York, NY, USA, 321-333. DOI: https://doi.org/10.1145/2984511.2984582

37. Eric Larson, Gabe Cohn, Sidhant Gupta, Xiaofeng Ren, Beverly Harrison, Dieter Fox, and Shwetak Patel. 2011. HeatWave: thermal imaging for surface user interaction. In Proceedings of the SIGCHI Conference on Human Factors in Computing Systems (CHI '11). ACM, New York, NY, USA, 2565-2574. DOI: https://doi.org/10.1145/1978942.1979317

38. Hanchuan Li, Can Ye, and Alanson P. Sample. 2015. IDSense: A Human Object Interaction Detection System Based on Passive UHF RFID. In Proceedings of the 33rd Annual ACM Conference on Human Factors in Computing Systems (CHI '15). ACM, New York, NY, USA, 2555-2564. DOI: https://doi.org/10.1145/2702123.2702178

39. Hanchuan Li, Eric Brockmeyer, Elizabeth J. Carter, Josh Fromm, Scott E. Hudson, Shwetak N. Patel, and Alanson Sample. 2016. PaperID: A Technique for Drawing Functional Battery-Free Wireless Interfaces on Paper. In Proceedings of the 2016 CHI Conference on Human Factors in Computing Systems (CHI '16). ACM, New York, NY, USA, 5885-5896. DOI: https://doi.org/10.1145/2858036.2858249

40. Hanchuan Li, Peijin Zhang, Samer Al Moubayed, Shwetak N. Patel, and Alanson P. Sample. 2016. ID-Match: A Hybrid Computer Vision and RFID System for Recognizing Individuals in Groups. In Proceedings of the 2016 CHI Conference on Human Factors in Computing Systems (CHI '16). ACM, New York, NY, USA, 4933-4944. DOI: https://doi.org/10.1145/2858036.2858209

41. Living Wall, Online Documentation. Retrieved January 5, 2018 from http://highlowtech.org/?p=27

42. Hui Liu, H. Darabi, P. Banerjee, and Jing Liu. 2007. Survey of Wireless Indoor Positioning Techniques and Systems. Trans. Sys. Man Cyber Part C 37, 6 (November 2007), 1067-1080. DOI: http://dx.doi.org/10.1109/TSMCC.2007.905750

43. Takuya Maekawa, Yutaka Yanagisawa, Yasue Kishino, Katsuhiko Ishiguro, Koji Kamei, Yasushi Sakurai, and Takeshi Okadome. 2010. Object-based activity recognition with heterogeneous sensors on wrist. In Proceedings of the 8th international conference on Pervasive Computing (Pervasive'10). Springer-Verlag, Berlin, Heidelberg, 246-264. DOI: http://dx.doi.org/10.1007/978-3-642-12654-3_15

44. Jon Moeller and Andruid Kerne. 2012. ZeroTouch: an optical multi-touch and free-air interaction architecture. In Proceedings of the SIGCHI Conference on Human Factors in Computing Systems(CHI '12). ACM, New York, NY, USA, 2165-2174. DOI: http://dx.doi.org/10.1145/2207676.2208368

45. Adiyan Mujibiya and Jun Rekimoto. 2013. Mirage: exploring interaction modalities using off-body static electric field sensing. In Proceedings of the 26th annual ACM symposium on User interface software and technology (UIST '13). ACM, New York, NY, USA, 211-220. DOI: http://dx.doi.org/10.1145/2501988.2502031

46. Lionel M. Ni, Yunhao Liu, Yiu Cho Lau, and Abhishek P. Patil. 2004. LANDMARC: indoor location sensing using active RFID. Wirel. Netw. 10, 6 (November 2004), 701-710. DOI: http://dx.doi.org/10.1023/B:WINE.0000044029.06344.dd

47. MG Chemicals. Product Information. Retrieved September 18, 2017 from http://www.mgchemicals.com/products/emi-and-rfi-shielding/acrylic-conductive-coatings-ar-series/838ar-total-ground-carbon-conductive-coating

48. MG Chemicals. Product Information. Retrieved September 18, 2017 from http://www.mgchemicals.com/products/emi-and-rfi-shielding/water-based-conductive-coatings-wb-series/841wb-super-shield-water-based-nickel-conductive-coating

49. MG Chemicals. Product Information. Retrieved September 18, 2017 from http://www.mgchemicals.com/products/emi-and-rfi-shielding/acrylic-conductive-coatings-ar-series/841ar-super-shield-nickel-conductive-coating

50. MG Chemicals. Product Information. Retrieved September 18, 2017 from http://www.mgchemicals.com/products/emi-and-rfi-shielding/water-based-conductive-coatings-wb-series/842wb-super-shield-water-based-silver-conductive-coating

51. O. Omojola, E. Rehmi Post, M. D. Hancher, Y. Maguire, R. Pappu, B. Schoner, P. R. Russo, R. Fletcher, and N. Gershenfeld. 2000. An installation of interactive furniture. IBM Syst. J. 39, 3-4 (July 2000), 861-879. DOI: http://dx.doi.org/10.1147/sj.393.0861

52. Sophocles J. Orfanidis Electromagnetic waves and antennas. New Brunswick, NJ: Rutgers University, 2002.

53. Joseph A. Paradiso, Kai-yuh Hsiao, Joshua Strickon, Joshua Lifton, and Ari Adler. "Sensor systems for interactive surfaces." IBM Systems Journal 39, no. 3.4 (2000): 892-914. DOI: https://doi.org/10.1147/sj.393.0892

54. Joseph A. Paradiso, Che King Leo, Nisha Checka, and Kaijen Hsiao. 2002. Passive acoustic knock tracking for interactive windows. In CHI '02 Extended Abstracts on Human Factors in Computing Systems (CHI EA '02).

ACM, New York, NY, USA, 732-733. DOI: http://dx.doi.org/10.1145/506443.506570

55. PJRC. Product Information. Retrieved September 18, 2017 from https://www.pjrc.com/teensy/teensy31.html

56. Qifan Pu, Sidhant Gupta, Shyamnath Gollakota, and Shwetak Patel. 2013. Whole-home gesture recognition using wireless signals. In Proceedings of the 19th annual international conference on Mobile computing & networking (MobiCom '13). ACM, New York, NY, USA, 27-38. DOI: http://dx.doi.org/10.1145/2500423.2500436

57. Tauhidur Rahman, Alexander T. Adams, Ruth Vinisha Ravichandran, Mi Zhang, Shwetak N. Patel, Julie A. Kientz, and Tanzeem Choudhury. 2015. DoppleSleep: a contactless unobtrusive sleep sensing system using short-range Doppler radar. In Proceedings of the 2015 ACM International Joint Conference on Pervasive and Ubiquitous Computing (UbiComp '15). ACM, New York, NY, USA, 39-50. DOI: https://doi.org/10.1145/2750858.2804280

58. Niranjini Rajagopal, Suman Giri, Mario Berges, and Anthony Rowe. 2013. A magnetic field-based appliance metering system. In Proceedings of the ACM/IEEE 4th International Conference on Cyber-Physical Systems (ICCPS '13). ACM, New York, NY, USA, 229-238. DOI: http://dx.doi.org/10.1145/2502524.2502555

59. Jun Rekimoto. 2002. SmartSkin: an infrastructure for freehand manipulation on interactive surfaces. In Proceedings of the SIGCHI Conference on Human Factors in Computing Systems (CHI '02). ACM, New York, NY, USA, 113-120. DOI: http://dx.doi.org/10.1145/503376.503397

60. Jun Rekimoto, and Nobuyuki Matsushita. "Perceptual surfaces: Towards a human and object sensitive interactive display." In Workshop on Perceptual User Interfaces (PUI'97), pp. 30-32. 1997.

61. Michael Rohs, and Beat Gfeller. Using camera-equipped mobile phones for interacting with real-world objects. na, 2004.

62. Anthony Rowe, Mario Berges, and Raj Rajkumar. 2010. Contactless sensing of appliance state transitions through variations in electromagnetic fields. In Proceedings of the 2nd ACM Workshop on Embedded Sensing Systems for Energy-Efficiency in Building (BuildSys '10). ACM, New York, NY, USA, 19-24. DOI: http://dx.doi.org/10.1145/1878431.1878437

63. Muhamad Risqi Utama Saputra, Guntur Dharma Putra, and Paulus Insap Santosa. "Indoor human tracking application using multiple depth-cameras." In Advanced Computer Science and Information Systems (ICACSIS), 2012 International Conference on, pp. 307-312. IEEE, 2012.

64. SciPy.org Retrieved September 19, 2017 from https://docs.scipy.org/doc/scipy/reference/optimize.html

65. Joshua R. Smith, Tom White, Christopher Dodge, Joseph Paradiso, Neil Gershenfeld, and David Allport. 1998. Electric Field Sensing For Graphical Interfaces. IEEE Comput. Graph. Appl. 18, 3 (May 1998), 54-60. DOI: http://dx.doi.org/10.1109/38.674972

66. Joshua R. Smith. 1999. Electric Field Imaging. Ph.D. Dissertation. Massachusetts Institute of Technology, Cambridge, MA, USA. AAI0800637.

67. Andrew Spielberg, Alanson Sample, Scott E. Hudson, Jennifer Mankoff, and James McCann. 2016. RapID: A Framework for Fabricating Low-Latency Interactive Objects with RFID Tags. In Proceedings of the 2016 CHI Conference on Human Factors in Computing Systems (CHI '16). ACM, New York, NY, USA, 5897-5908. DOI: https://doi.org/10.1145/2858036.2858243

68. Shih-Wei Sun, Chien-Hao Kuo, and Pao-Chi Chang. 2016. People tracking in an environment with multiple depth cameras. J. Vis. Comun. Image Represent. 35, C (February 2016), 36-54. DOI: https://doi.org/10.1016/j.jvcir.2015.11.012

69. Miika Valtonen, Jaakko Maentausta, and Jukka Vanhala. 2009. TileTrack: Capacitive human tracking using floor tiles. In Proceedings of the 2009 IEEE International Conference on Pervasive Computing and Communications (PERCOM '09). IEEE Computer Society, Washington, DC, USA, 1-10. DOI: https://doi.org/10.1109/PERCOM.2009.4912749

70. Miika Valtonen, Lasse Kaila, Jaakko Mäentausta, and Jukka Vanhala. 2011. Unobtrusive human height and pose recognition with a capacitive sensor. J. Ambient Intell. Smart Environ. 3, 4 (December 2011), 305-332. DOI: http://dx.doi.org/10.3233/AIS-2011-0120

71. Cati Vaucelle, Hiroshi Ishii, and Joseph A. Paradiso. 2009. Cost-effective wearable sensor to detect EMF. In CHI '09 Extended Abstracts on Human Factors in Computing Systems (CHI EA '09). ACM, New York, NY, USA, 4309-4314. DOI: https://doi.org/10.1145/1520340.1520658

72. Jue Wang, Deepak Vasisht, and Dina Katabi. 2014. RF-IDraw: virtual touch screen in the air using RF signals. SIGCOMM Comput. Commun. Rev. 44, 4 (August 2014), 235-246. DOI: https://doi.org/10.1145/2740070.2626330

73. Joey Wilson and Neal Patwari. 2010. Radio Tomographic Imaging with Wireless Networks. IEEE Transactions on Mobile Computing 9, 5 (May 2010), 621-632. DOI: http://dx.doi.org/10.1109/TMC.2009.174

74. Andrew Wilson and Hrvoje Benko. 2010. Combining multiple depth cameras and projectors for interactions on, above and between surfaces. In Proceedings of the 23nd annual ACM symposium on User interface software and technology (UIST '10). ACM, New York, NY, USA, 273-282. DOI: https://doi.org/10.1145/1866029.1866073

75. Andrew Wilson, Hrvoje Benko, Shahram Izadi, and Otmar Hilliges. 2012. Steerable augmented reality with the beamatron. In Proceedings of the 25th annual ACM symposium on User interface software and technology (UIST '12). ACM, New York, NY, USA, 413-422. DOI: https://doi.org/10.1145/2380116.2380169

76. Robert Xiao, Chris Harrison, and Scott E. Hudson. 2013. WorldKit: rapid and easy creation of ad-hoc interactive applications on everyday surfaces. In Proceedings of the SIGCHI Conference on Human Factors in Computing Systems (CHI '13). ACM, New York, NY, USA, 879-888. DOI: https://doi.org/10.1145/2470654.2466113

77. Robert Xiao, Greg Lew, James Marsanico, Divya Hariharan, Scott Hudson, and Chris Harrison. 2014. Toffee: enabling ad hoc, around-device interaction with acoustic time-of-arrival correlation. In Proceedings of the 16th international conference on Human-computer interaction with mobile devices & services (MobileHCI '14). ACM, New York, NY, USA, 67-76. DOI: http://dx.doi.org/10.1145/2628363.2628383

78. Robert Xiao, Gierad Laput, Yang Zhang, and Chris Harrison. 2017. Deus EM Machina: On-Touch Contextual Functionality for Smart IoT Appliances. In Proceedings of the 2017 CHI Conference on Human Factors in Computing Systems (CHI '17). ACM, New York, NY, USA, 4000-4008. DOI: https://doi.org/10.1145/3025453.3025828

79. Chouchang Yang, and Alanson P. Sample. "EM-ID: Tag-less identification of electrical devices via electromagnetic emissions." In RFID (RFID), 2016 IEEE International Conference on, pp. 1-8. IEEE, 2016. DOI: https://doi.org/10.1109/RFID.2016.7488014

80. Moustafa Youssef, Matthew Mah, and Ashok Agrawala. 2007. Challenges: device-free passive localization for wireless environments. In Proceedings of the 13th annual ACM international conference on Mobile computing and networking (MobiCom '07). ACM, New York, NY, USA, 222-229. DOI: http://dx.doi.org/10.1145/1287853.1287880

81. Yang Zhang, Gierad Laput, and Chris Harrison. 2017. Electrick: Low-Cost Touch Sensing Using Electric Field Tomography. In Proceedings of the 2017 CHI Conference on Human Factors in Computing Systems (CHI '17). ACM, New York, NY, USA, 1-14. DOI: https://doi.org/10.1145/3025453.3025842

82. Nan Zhao, Gershon Dublon, Nicholas Gillian, Artem Dementyev, and Joseph A. Paradiso. "EMI Spy: Harnessing electromagnetic interference for low-cost, rapid prototyping of proxemic interaction." In Wearable and Implantable Body Sensor Networks (BSN), 2015 IEEE 12th International Conference on, pp. 1-6. IEEE, 2015. DOI: https://doi.org/10.1109/BSN.2015.7299402

83. Thomas G. Zimmerman, Joshua R. Smith, Joseph A. Paradiso, David Allport, and Neil Gershenfeld. 1995. Applying electric field sensing to human-computer interfaces. In Proceedings of the SIGCHI Conference on Human Factors in Computing Systems (CHI '95). ACM Press/Addison-Wesley Publishing Co., New York, NY, USA, 280-287. DOI: http://dx.doi.org/10.1145/223904.223940